TSINGHUA SCIENCE AND TECHNOLOGY
ISSN 1007-0214 06/20 pp698–720
DOI: 10.26599/TST.2023.9010065
Volume 29, Number 3, June 2024

Cooperative Spectrum Sensing Deployment for Cognitive Radio Networks for Internet of Things 5G Wireless Communication

Thulasiraman Balachander, Kadiyala Ramana, Rasineni Madana Mohana, Gautam Srivastava*, and Thippa Reddy Gadekallu

Abstract: Recently, Cooperative Spectrum Sensing (CSS) for Cognitive Radio Networks (CRN) plays a significant role in efficient 5G wireless communication. Spectrum sensing is a significant technology in CRN to identify underutilized spectrums. The CSS technique is highly applicable due to its fast and efficient performance. 5G wireless communication is widely employed for the continuous development of efficient and accurate Internet of Things (IoT) networks. 5G wireless communication will potentially lead the way for next generation IoT communication. CSS has established significant consideration as a feasible resource to improve identification performance by developing spatial diversity in receiving signal strength in IoT. In this paper, an optimal CSS for CRN is performed using Offset Quadrature Amplitude Modulation Universal Filtered Multi-Carrier Non-Orthogonal Multiple Access (OQAM/UFMC/NOMA) methodologies. Availability of spectrum and bandwidth utilization is a key challenge in CRN for IoT 5G wireless communication. The optimal solution for CRN in IoT-based 5G communication should be able to provide optimal bandwidth and CSS, low latency, Signal Noise Ratio (SNR) improvement, maximum capacity, offset synchronization, and Peak Average Power Ratio (PAPR) reduction. The Energy Efficient All-Pass Filter (EEAPF) algorithm is used to eliminate PAPR. The deployment approach improves Quality of Service (QoS) in terms of system reliability, throughput, and energy efficiency. Our in-depth experimental results show that the proposed methodology provides an optimal solution when directly compares against current existing methodologies.

Key words: cooperative spectrum sensing; cognitive radio network; Internet of Things; offset quadrature amplitude modulation; universal filtered multi-carrier; non-orthogonal multiple access

1 Introduction

In any efficient 5G communication using Cognitive Radio Networks (CRN), Spectrum Sensing (SS) is used to determine accessibility in frequency resources. The

• Thulasiraman Balachander is with SRM Institute of Science and Technology, Tamil Nadu 603203, India. E-mail: balachat2@srmist.edu.in.
• Kadiyala Ramana is with Lebanese American University, Beirut 1102, Lebanon, and also with Chaitanya Bharathi Institute of Technology, Hyderabad 500075, India. E-mail: ramana.it01@gmail.com.
• Rasineni Madana Mohana is with Chaitanya Bharathi Institute of Technology, Hyderabad 500075, India. E-mail: rmmnaidu@gmail.com.
• Gautam Srivastava is with Brandon University, Brandon, R7A 0A1, Canada, China Medical University, Taichung 404327, China, and Lebanese American University, Beirut 1102, Lebanon. E-mail: srivastavag@brandonu.ca.
• Thippa Reddy Gadekallu is with Department of Electrical and Computer Engineering, Lebanese American University, Beirut 1102, Lebanon. E-mail: thippareddy.g@vit.ac.in.
* To whom correspondence should be addressed.
Manuscript received: 2022-12-12; revised: 2023-06-08; accepted: 2023-06-17

notion of fixed (or static) frequency allocation underpins the majority of today's wireless communication technologies. They are programmed to function in specific frequency bands. This fixed allotment leads to poor spectrum usage particularly during periods of low congestion. Some assigned frequency bands are used less than 15% of the time. Furthermore, there has been a lot of advancement of 5G efficient wireless communication technology solutions. Moreover, the enormous increase in the number of linked devices through protocol-based Internet of Things (IoT) networks, and topology-based Wireless Sensor Network (WSN) technologies with subsequent accurate wireless utilization, force the wireless communication society to improve the utilization of narrow bandwidth resource base to meet the growing requirement on wireless technology[1]. SS allocation's real-time characteristic and performance as well as the energy spectrum access method founded on the master-slave balancing adaptive deployment paradigm have been investigated in the literature. Based on the requirement for convergence speed and migration patterns, our methodology creates a new encryption technique for use. The reactivity community can be estimated with only a few computational nodes at identical intervals to improve calculation performance[2]. Cooperative Spectrum Sensing (CSS) is a hot topic because it has the potential to address the concealing endpoint problem. CSS's sensing capability, on the other hand, is still lacking, particularly in low Signal Noise Ratio (SNR) conditions. Convolutional Neural Networks (CNN) are thought to extract characteristics from an observed signal and enhance sensing performance. More precisely, a unique 2D database of the received data is created, and three traditional CNN-based CSS methods (LeNet, AlexNet, and VGG-16) are developed and evaluated on the database[3]. CSS is thought to be a strong tool for maximizing the use of restricted available spectrum. If CSS reflects that practically all users on secondary units may be reliable, hackers may be able to execute cognitive radio data manipulation operations. Current initiatives have been devoted to building trust structures to combat such a danger. However, certain hackers can create a cluster-based collusive group and consequently cause issues using Spectrum Sensing Data Falsification (SSDF) attacks. The defence mechanism against such attacks using XDA from the standpoint of XOR range evaluation is presented to inhibit a collusive SSDF attack, taking into account the polarity of sensing data. The XOR similarity computation based on previous binary (0 and 1) detecting data is utilized XDA to quantify the resemblance[4]. There are several SS approaches offered with the most prominent matched filter detection, Cyclostationary feature identification, and energy detection. Compared to other detection approaches, energy detection is well-known for its simplicity and lack of pre-existing information on the Primary User (PU) signal. The detection performance in SS can be decreased due to a variety of issues such as multipath fading, shadowing, and the noise uncertainty problem. CSS techniques have been developed to mitigate these effects.

The CRN accessibility technique is shown in Fig. 1. With full-duplex mode and half-duplex, it incorporates underlying, overlaying, and interweaving categorization. Improving Energy Efficiency (EE) and High Scalability (HS) in 5G wireless communication systems is a major task capable of meeting upcoming wireless communication demands and delivering Quality of Service (QoS) requirements including allowing for maximum bandwidth with low energy consumption. In this paper, a look-up table is used to allow a fuzzy-based technique to study SS and EE difficulties in 5G technology and achieve an optimally balanced trade-off among them to improve the overall system performance[5].

Downlink Cognitive Radio (DCR) has the potential to alleviate spectrum shortages by allowing commercial wireless sensor networks to use common carrier frequency capabilities to extend their bandwidth. Overlay CR equipment, on the other hand, could be accomplished by correctly altering wireless communication settings in response to wireless network sensing. In Ref. [6], two alternative SNR estimate techniques for spatial-temporal interleaved data expectations triggered by CRN-based viable IoT are presented to achieve this aim. Roads are split into equal parts and sub-segmented according to the likelihood value. Normal vehicles or spectrum allocation create local development issues by utilizing a hybrid Machine Learning (ML) approach that incorporates fuzzy and native Bayes techniques to choose the best SS method. The sensing approaches employ adaptive thresholds. In Ref. [7], a segmented

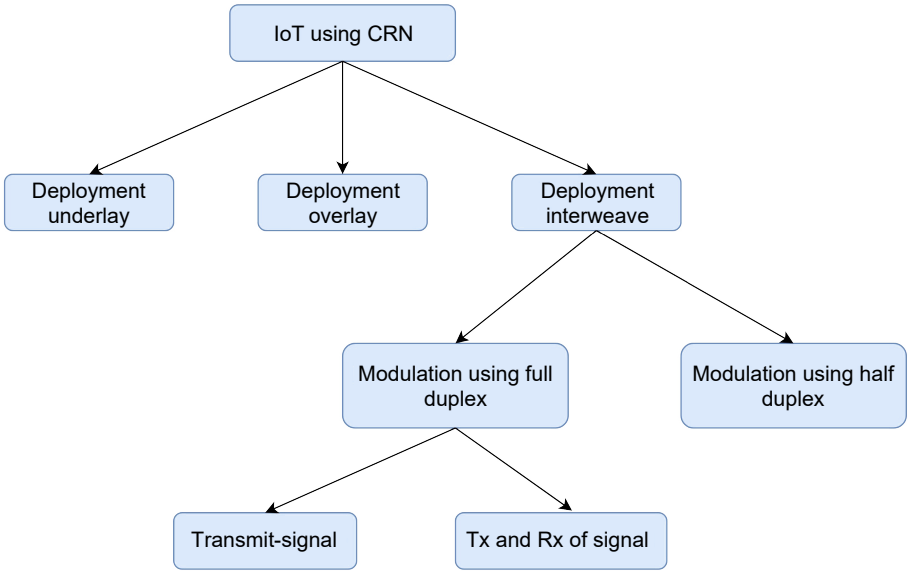

Fig. 1 CRN accessing paradigm.

spectrum operator in cooperation with SS is used with the tri-agent supervised learning method to make a general choice. In CRN, CSS methods termed Demodulate Cooperative Spectrum Sensing (DCSS) and Modulate Cooperative Spectrum Sensing (MCSS) are developed.

The following are the major aims and implementation of our developed system-based cooperative spectrum sensing schemes:

- To use strategies to address the problem of increased transmission requirement in a maximum likelihood method. Moreover, the effect of reflecting users' power level, which is defined by the interruption limitation, on CSS methods' structural characterization is examined.
- To use the work in Ref. [8], in relation to predictive performance and interruption likelihood, evaluate the sensing effectiveness of our proposed CSS methods. Under the practicality of static structural systems, conditions were investigated for the Likelihood of Spectral Utilization (LSU) of a CR system with soft CSS.

The duration of a period in practical applications is typically set, with the period consisting of detecting, monitoring, and communication periods. Consequently, in CSS, raising the sensing and transmitting time length enhances the probability of successfully detecting PU relative importance while decreasing the transmitting processing time, resulting in lower bandwidth[9].

Cognitive radio is a powerful platform that may be used in WSN to enhance spectrum utilization. A system architecture incorporates advancements at the lower levels of a CRN of WSN with CRN functionality for productive wireless device energy harvesting, resource channel handoffs complete removal, and effective energy storage with improvement in QoS of information frequency wireless device implementations via CRN streams. For energy efficiency, any massive WSN is split into groups, each of which connects to a cloud-assisted General Processor (GP)[10]. Sensor Nodes (SN) allow bidirectional interaction for communication between two principal users in a combination of sensor nodes' primary users. In exchange, SN gather energy from primary users' transmissions and utilize the gained energy to power their transmissions. Input and output connections among the primary side PU and directional data gathering among sensor devices may be accomplished in three stages in such a system. For simultaneous wireless data and power transmission, a power partitioning method is used.

SN broadcast primary and secondary signals using the Amplify and Forward (AF) method, while the PU uses decision mixing to acquire the available direct relationship[11]. The perceptual connectivity-powered wireless medium is made up of an important communication pair and a secondary communication network intended for IoT. For the information handover of the second communication network, a unique hybrid production and backscatter transmission method is proposed. Once the principal network is overfilled, Perceptive Users (PEU) employ

conservation Back Scatter mode to backscatter the intrusive information through the Key Spreader (KS) for gathering information and preserving power for upcoming information communication. Any secondary user request can be given, and Cognitive Users (CU) reversely disperse the intercepted signal from the energy transmitter in the Bi-static Scattering (BS) phase or operate in the function to transfer signals[12].

The level of expansion of IoT wireless networking technology is seen in Fig. 2. A novel energy detection technique is suggested that is based on temporal data potential identification. A more realistic 2D Cognitive WSN (CWSN) architecture prototype is developed to evaluate the method's feasibility and reliability, in which the key indication source could be dispersed by a particular sensing region arbitrarily cycle. Thus, the application of any specific fusion technique for 2D sensor devices contains 2 significant identifying phases: (1) spectral detection non-cooperation for all device nodes, and (2) position prediction with range fusion of chosen sensor node. Another point to consider is the energy constraint in CWSN[13]. In energy storage for CRN, the system utility maximization issue is addressed. Sensor nodes in Cognitive Radio Sensor Networks (CRSN), unlike typical sensor nodes, have incorporated multiple access modules, allowing them to automatically access licensed frequencies.

Due to the importance of flexible data transmission in ensuring network infrastructure for CRSN, integrated models that do not address flexible communication links cannot be easily implemented. To do this, issues with exploiting system efficacy by adapting model proportions and network capability of the device while keeping energy usage, available bandwidth, and disturbance restrictions in mind[14]. In WSN, the efficiency of multi-hop adaptive wireless enabled Device-to-Device (D2D) interactions is very important. According to our observations, each SN gathers energy from several reliable electricity signals and uses subsurface cognitive radio to share spectral efficiency with multiple Primary Receptions (PR). Consider a real-world situation of adaptive connectivity D2D communications in WSN in which obstruction channel information is considered to be poor. In this paper, we present two user optimization techniques, specifically Dual-Hop Sequencing (DHS) and highest-quality programming both used to increase the performance of the network[15]. The technique addresses the problem of dropping drive depletion and increasing system lifecycle in a wireless device system based on sensors that could be made up of arbitrarily oriented devices that conduct inter CSS. More specifically, a deterministic technique is proposed for assessing the CWSN duration while also considering detection quality.

The variety of devices and principal users in the region are found to take two-dimensional Gaussian probabilities, while detection and false alarm probabilities for the devices are computed

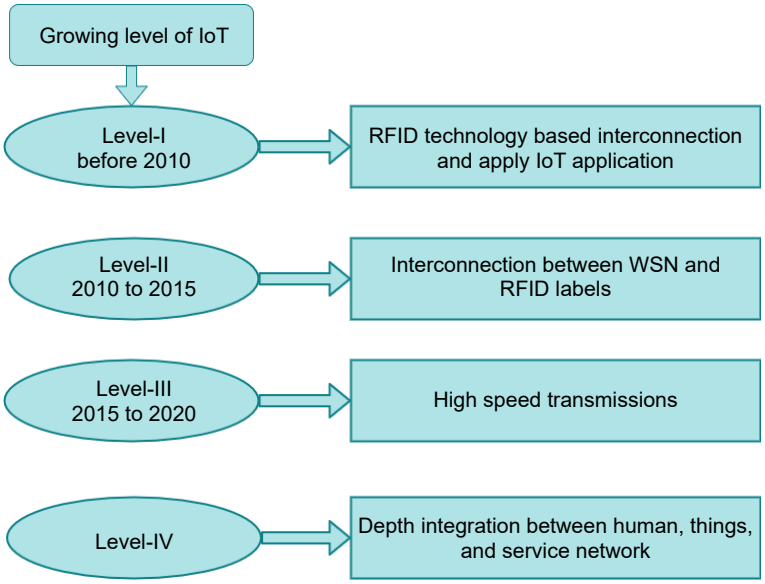

Fig. 2 Level growth of IoT technology.

objectively[16]. Different distributions have become severely scarce as mobile communication offerings and wireless technologies have developed. Enterprise WSN (EWSN) may be required to take radio frequencies with other devices, resulting in significant interruption. Industrial Cognitive Radio Networks (ICRN) are created to solve this, and signal categorization is a basic and crucial concept mainly for manufacturing industrial system wireless networks that are a necessity to recognize distrustful signals. In Ref. [17], an innovative context for data intelligence categorization development of deep learning systems is suggested.

Even though traditional WSN nodes merely detect the surroundings, recent developments in WSN, such as Perceptual (P-WSN), wireless sensing element network, wireless action network, and encryption in WSN need networks to perform computations. Furthermore, most elevated techniques are discarded for next-generation WSN without examination into resource restrictions in nodes and a lack of an assessment mechanism. Many sources, for example, have recommended a low-performance, reduced Energy Detection (ED) technique for CWSN without any assessment or analysis, based only on the fact that ED has the least difficulty of all energy detection techniques, as was seen in Ref. [18]. An Internet Protocol's main purpose is end-to-end traffic regulation, which aims to determine how much traffic flow provided by the resource can be managed by the system. Even though a lot of research is present in the literature to oppose the end-to-end protected transmitting issue in traditional WSN, due to the non-assorted range, these strategies typically result in an extended interruption for the base station to react to traffic delays in wireless communication adhoc connections. As a result, the end-to-end bandwidth drops significantly[19]. Non-licensed spectrum utilization of Secondary Users (SU) must precede cognizance for extended periods throughout that can consume the energy spectrum in CRN to maximize the utilization of idle times on primary channels. As a result, researchers tend to concentrate on the issue of how long an SU can retain a primary channel as well as the average quantity of data that can be transferred throughout that period. Situations with similar and non-similar data confirmation for different quantities of SU may be done conditionally on the movement stages of spectrum utilization PU. In Ref. [20], the authors developed security through numerical equations to compute the resulting interpretations for all examined cases to reduce calculating difficulty.

The OQAM/UFMC/NOMA technique is used to get the best CSS for CRN. Spectrum availability and bandwidth usage are two major issues in CRN for IoT 5G wireless technology. CRN for IoT-based 5G communication should be optimized to offer optimal throughput and CSS, low latency, improved SNR, maximum capacity, offset synchronization, and reduced Peek to Arerage Power Ratio (PAPR), among other things. The closed-form of important QoS variables such as structure dependability, maximization of throughput, and network energy efficiency is accomplished using the objective function.

The rest of the paper is organized as follows. In Section 2, various related research articles and papers are discussed. In Section 3, secured CSS is discussed. In Section 4, the system model, QoS Requirements for IoT Systems, Practical Considerations, optimal utilization of CSS, CRN using OQAM/UFMC/NOMA for IoT, and accurate gathering of data in CRSN are developed. Our in-depth experimental results and discussion are given in Section 5. Finally, the conclusion is given in Section 6.

2 State of the Art for Cognitive Radio Network in IoT 5G Wireless Communication

Li et al.[21] investigated the fundamental contexts with possible insight into perceptive IoT. The low bandwidth issue is solved through additional features of efficient IoT. IoT modules are often highly functional, resulting in trade-offs with several bandwidth-request technologies in competition with each other for efficiency.

Osman and Zaki[22]introduced an interference control model for CRN. This proposed model uses the Lagrangian objective function to decrease interference and enhance efficient energy productivity and dependability with accurate IoT communication systems using 5G communication networks. Moreover, methodologies to control interference between IoT and Base Stations are examined. To accomplish the provided model's goal, first the authors designed a multi-objective optimization technique. The restricted nature of important QoS characteristics such as system dependability, bandwidth, and energy consumption

were then investigated based on an objective function.

Baniata et al.[23] investigated an energy-efficient clustering approach for MIMO-based IoT communications networks. For IoT applications in 5G environments and beyond, the authors proposed an innovative MIMO-based energy-harvesting irregular fusion gathering method. The efficacy of the proposed MIMOHC protocol is evaluated using different techniques and compared to their defined current framework.

Al-kahtani et al.[24]presented a hybrid resource mass and energy efficient technique for a mobile device-to-device data communication system that uses successive interference cancellation which is responsive to the Regular Water Filling (RWF) methodology as a portion of the control distribution solution. When compared specifically to a Sequential Iterative Water-Filling (SIWF) power allocation methodology, the SIWF-based spatial domain frequency division multiple access methods provide better energy efficiency.

Sahoo et al.[25] developed a two-stream spectrum hopping procedure both with and without global channel estimation for ICRN to maximize the degree of docking in the shortest possible time, minimize Inter-Docking Increments, and decrease Mean Time To Resolve (MTTR) by 2 Parallel Secondary Users (PSU). Establishing the communication protocol through this spectrum hopping approach in ICRN, on the other hand, is a fairly tough task. Effective channel hopping algorithms must be devised to ensure dependable throughput in ICRN.

Gallardo et al.[26] tackled the problem of constant processing data in a multi-hop, multi-transceiver CRN where channel access is governed by an empty Time Division Multiple Access (TDMA) standard and the primary usage data is an ON/OFF procedure. Moreover, the issue of finding available end-to-end throughput for load balancing has been proven to be NP-complete. Therefore, instead of concentrating on a probability distribution function and examining its worst-case performance, by simplifying the problem of continuous processing requests by employing a randomly selected scheduling scheme and evaluating its average performance, strong results were achieved.

Patel et al.[27]resolved the issue of CSS in multi-user MIMO CRN where Channel State Information (CSI) generated by the transceiver of the SU channels accessible on combination midpoint was indefinite. Numerous approaches remain to be obtainable that uses mutual exclusion instructions founded on resident scheme selections that are communicated through an orthogonal data transmission channel by participating nodes. For both opposing and non-orthogonal signals, fusion rules are first generated at the fusion center under perfect CSI.

Xu et al.[28]investigated uplink authentication proportional equality power and the sub-route optimization problem for perceptual sensor networks with inter-network collaboration. Allowing inexact spectral detecting and network state data, each SU creates variations in receiver influence and sub-channels to enhance secrecy while following set QoS boundaries. The double decomposition approach is used to provide optimum information preservation and sub-network energy distribution to challenge the above-mentioned bi-convex optimization problem.

3 Cooperative Spectrum Sensing

A concurrent fusion network may be used to mimic the CSS procedure. Autonomous sensing, data analysis, and data aggregation are all controlled by central identification known as the Fusion Center (FC). To begin, each SU uses energy monitoring to detect a PU's signal through the efficient spectrum detection network channel that could be a licensed user frequency band in which a layer-based physical end-to-end link exists among the PU spreader and each SU for the persistence of observing the central energy spectrum.

The NOMA orthogonal slot allocation's benefit of increased energy efficiency comes with the drawback of limiting the number of customers who can access the system. Take into account a NOMA-CRN with K SU_s and J transmitter-receiver pairs. The k^{th} secondary user and the j^{th} pair of principal transmitter-receiver links, respectively, are denoted by the variables S_k and P_j, respectively. The major links in the suggested model are both potentially active and always protected. The secondary network is a single cellular network with all SU having TDMA uplinks to the secondary base station, while the primary network is made up of J transmitter-receiver pairs and uses a non-orthogonal SCMA-based allocation scheme for slots.

All SU communicate specific sensing data to FC through the development of processes, which is a control channel with a direct point-to-point link between each SU and FC. Finally, to identify the existence of PU, FC combines the incoming individual

sensory data into a single judgement value. Three common data fusion rules may be used to make such a final decision: the AND, OR, and Majority procedures. The AND rule requires all SU to observe the channel as idle, the OR rule requires at least one SU to observe the channel as idle, and finally the Majority rule requires a minimum of half of the SU to observe the channel as idle. These rules are used in cooperative sensing methods in CRNs to make binary decisions on whether the channel is idle or busy based on the observations of multiple SU. The energy spectrum detection technique usually does not detect a PU signal, then each data sensing for the energy detection technique could also be seen as a binary hypothesis problem using Eqs. (1) and (2).

$$f(t) = a(t), \qquad X_0 \tag{1}$$

$$h(t) = u(t) + a(t), \qquad X_1 \tag{2}$$

where $f(t)$ is the identified data at every secondary user, $u(t)$ is the encoded primary user data, $h(t)$ is the signal detecting channel gain, $a(t)$ is the zero variance Gaussian multiplicative noise, and t is the measurement index, respectively. The hypotheses of the PU signal's nonexistence and existence, respectively, are represented by X_0 and X_1, respectively. If $f(t)$ is greater than the spectrum sensing threshold value, the presence of PU can be communicated. Aside from that, no primary user data is observed. The detecting information of each SU is obtained after the unique sensing. SU_i's sensing data is represented by d_i, which is a categorical variable in general as in Eq. (3).

$$V = 0, X_0 = 1, \qquad X_1 \tag{3}$$

where 0 and 1 denote the notion of PU spectrum status nonexistence and presence, respectively. As a result of the data synthesis, FC's ultimate conclusion is likewise binary. The AND, OR, and Majority rules are typical cooperative sensing methods in CSS. When all $d_i = 1$, FC uses the AND rule to make $d = 1$. When one $d_i = 1$, the OR rule relates to $d = 1$. According to the Majority criterion, a minimum of half of the secondary users should provide 1.

In NOMA communication, XOR is a common Boolean logic operation that is used to provide parity bits for error checking and fault tolerance. Two input bits are compared via XOR, which produces one output bit. The reasoning is clear. If the bits match, the outcome is 0. When the bits vary, the outcome is 1.

The OR approach works well when the amount of secondary users is large, while the AND instruction works well when the amount of cooperative SU is less in amount. In the scenario $\frac{kN}{2}$, the Majority principle may be obtained from the k out of N principle. E-commerce, P2P networks, adhoc networks, online social groups, and other situations have all benefited from these trust mechanisms.

3.1 Secured cooperative spectrum sensing from spectrum sensing data falsification attack

Currently, trust mechanisms are also important in the CSS world. The following are some examples of CSS trust mechanism systems. With the Beta reputation, a CSS technique is suggested. They do, however, need the base station to give its detecting consequence for the faith familiar sensing outcome gathering at each effective CSS movement that could place the base station under a lot of pressure if it also has to identify the PU signal at each effective CSS operation. To counter the SSDF threat, a safe CSS method is presented with the help of trustworthy SU. However, the amount of probability theory and statistics needed to identify hackers can increase computational efficiency. A perception method known as the weighted successive likelihood ratio test is used during the implementation of the technique which automatically includes the location of PU and SU to obtain approximately desirable subsequent likelihood. Moreover large sample sizes, which, in the worst-case scenario, could result in an impasse with infinite sensing sampling, are utilized. A multi-factor trust management system is proposed that includes several decision factors such as the background trust system, active element, motive factor, and integrity factor. However, evaluating these elements requires additional numerical simulation.

To minimize significant overload while still suppressing collusive SSDF attacks, we devise a compact collusive SSDF intruder identification technique based on lowering the computational difficulty of the trust mechanism. Because SU sensing data may be regarded as a binary variable (0 or 1), they can easily create two sorts of sensing outcomes: honest or false. The XOR length assessment design approach can be built on a random variable to prevent collusive SSDF threats. As a result of the rapid XOR operation

used on the 0 and 1 data acquired, the created approaches may be light, with collusive SSDF intruders being detected as SU with the smallest XOR duration and the highest importance. It may also make used of a fundamental trust processing method based on device values called Basic, in which each SU's trust value is initialized by 2 factors: (1) the quantity of honest detecting (hon) and (2) the rate of false detecting (fal). This specification might be enhanced by restricting the expansion of hon after discovering collusive SSDF operators. In reality, one of the most common designs for determining trust level using quantitative information is the Beta component (i.e., positive or negative). It looks at how many positive and negative actions a user has been involved in and then uses the beta probability density function to calculate the amount of confidence as in Eq. (4).

$$B(a,b) = T(a+b)a - 1(1)b - 1(\theta)\mathrm{Te}(a)\mathrm{Te}(b) \quad (4)$$

where θ is the likelihood of performances, $0 \leqslant \theta \leqslant 1$, $a > 0$, $b > 0$. $\mathrm{Te}(n) = (n-1)$ when n is a number. 1(1) represents the quality of honest detecting.

For instance, the i^{th} secondary user ($\mathrm{SU_{itr}}$), where hon and fal denote the amount of honest (positive) and false (negative) perceiving followed by SU_i, respectively. The initial assessment of $\mathrm{SU_{itr}}$'s trust model is as in Eq. (5).

$$\mathrm{Thi} = B(\mathrm{hon}+1, \mathrm{fal}+1) \quad (5)$$

Thi represents threshold which is equal to honest detection and false detection. As a result, the beta collecting anticipation rate is $E[\mathrm{Beta}(a,b)] = a/(a+b)$. In this situation, Thi can be calculated further as in Eq. (6).

$$\mathrm{Thi} = 1 + \mathrm{hon}_2 + \mathrm{hon}_1 + \mathrm{fal} \quad (6)$$

Let us call the trust value threshold δ. $\mathrm{SU_{itr}}$ will be recognized as an intruder if Thi is greater than or equal to δ, and vice versa. δ should meet two conditions to ensure CSS efficiency:

(1) As Thi$[0,1]$, then δ should be a reasonable number between 0 and 1;

(2) The value of δ can be changed to prevent fraudulent replies from being created by intruders submitting fake sensed information.

In $[0,1]$, δ definitely cannot be assigned to a limited quality. If this were done, hackers with a high trust value would have more chances to provide fake sensed information, leading to the most harmful replies. Furthermore, because of deep masking and multi-path fading, δ may not be established as the maximum trust rate since honest secondary users may deliver wrong sensed data with a lower likelihood. The simulation technique is an excellent choice for determining the reasonable value of δ.

3.2 Objective

Increased network performance, reduced latency, great efficiency, and significant machine-to-machine interactions are all features of 5G mobile communication networks. In this regard, one of the main research challenges for 5G is the creation of the multi-carrier waveform. To address the aforementioned issue, some advanced work suggests OQAM/UFMC/ NOMA as an alternative to the OFDM waveform. Indeed, some real-time communication techniques used in 4G networks made use of OFDM. Yet, it is unclear how it will be implemented in upcoming 5G networks. This is because using OQAM/NOMA for more recent wireless communications is unfeasible due to the strict requirements of 5G communications networks, which may be extended to effective 5G communications networks. To meet the requirements of upcoming communications systems, MCW with more versatility are urgently required. In terms of a low PAPR, synchronization, improved spectrum efficiency, and throughput, the proposed OQAM/UFMC/NOMA satisfies 5G capabilities. The OQAM/UFMC/NOMA proposed in this study make use of frequency mobility using the Energy Efficient All-Pass Filter (EEAPF) of the input signal to the universal filtered multi-carriers (UFMC) modes, as well as power-domain combining techniques like non-orthogonal multiple access (NOMA). The equivalent probability density function is used to conduct a statistical study of the PAPR.

4 Cognitive Radio Network Model for Internet of Things 5G Wireless Communication

CR technology is anticipated to be used in IoT architecture with modules. As a result, consumers may make use of any accessible spectrum. Primary users have exclusive operating privileges in permitted frequencies. The underutilized frequency range will be used by 5G NOMA CRN communication networks to improve bandwidth and address issues of spectrum scarcity for the predicted billions of IoT-connected devices on the forefront of networks, the ability to

detect accessible frequencies and underutilized spectrum, and finally by sensing the surrounding spectrum surroundings. CR will decide if a specific band is active or inactive at a specific time and place. Smart 5G architecture for IoT is homogeneous, enabling coverage for CR-enabled 5G communication networks everywhere. It will be able to handle a large number of connected devices as well as a diverse application server. It can also achieve greater capacity utilization, enhance network performance, minimize energy consumption, and show increased system throughput since it can employ all non-contiguous spectrums.

We assume that all SU are deployed separately and equally, with the same measurement of SNR of the sensing network in the primary signal's transmission range. Due to its simple structure and lack of requirement for previous information on the source signal and channel fading, an ED approach is assumed for spectrum sensing. Soft CSS is utilized in the CR network, in which each SU collects a set number of samples and then sends the potential speed of the gathered information to FC in numerous bits. The FC then adds together all SU provided numbers and makes a judgement by matching the total to a predetermined threshold level. Another expectation is that all SU send their data to FC in a NOMA way through the development of processes.

Figure 3 depicts the proposed CR network's structural system, in which a period (time) for SU is separated into three sections based on the number of steps performed by SU. Sensing time (T_s), reporting time (T_r), and transfer rate (T_{tr}) are the three parts of a period. $T = T_s + T_r + T_t$ is used for calculating the duration of a period. The sending time is defined by the number of Secondary users (multiple), the amount of

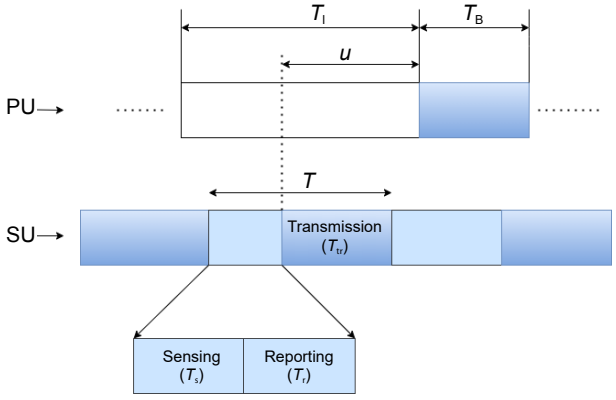

Fig. 3 Proposed CR network's structural system.

sending bits (N), and the sample rate of the ratings provided (fr). As a result, $T_r = \mathrm{IB}$ may be used to describe the reporting time. The time frame may now be represented using Eq. (7).

$$T = T_s + \mathrm{IB} + T_{tr} \tag{7}$$

T_I and T_B represent the idle and busy multi-step process of PU, respectively. A Poisson distribution regulates the movement of PU from occupied to idle and vice-versa. The incidence of certain occurrences at a particular rate although entirely nonlinear similar to a Poisson distribution. It is known that PU has two states in the spectral range, i.e., busy or idle, but the order in which these states appear is entirely arbitrary. As a result, the behaviour of PU's state transition may be described as a Poisson distribution by looking at its behaviour. As a result, T_I and T_B may both be represented as exponential distributions.

4.1 QoS requirements for IoT systems

Data rate, latency, and dependability are just a few of the QoS criteria for IoT applications. Furthermore, because of the widespread distribution of IoT sensing nodes, economics with environmental effects could be taken into account while designing IoT devices. To guarantee QoS from beginning to end, an IoT technology allocation technique for uplink and downlink resources is used. The required QoS for various IoT services is provided by the CR network. The usage of high-bandwidth communication channels is the primary strategy for ensuring QoS. The reason may be an increase in operating prices would raise the total charge of the IoT device and a rise in total consumption of energy is estimated as a large environmental concern because it is connected to greenhouse emissions implicitly.

Let SC denote the IoT system's collection of classification services. The following QoS characteristics apply to each class in SC: Data Rate (DR), Latency (L), Reliability (RE), Economic Effect (EC), and Environmental Impact (EI). It explores a restricted collection of service classes with quality of service measurement parameter characteristics that are shown in Table 1 to avoid losing generality and for demonstration reasons. For illustrative reasons, these characteristics are ranked from 0 to 3 in terms of importance, with 0 being least important, 1 being important, 2 being most important, and 3 being essential.

Table 1 Characteristics of OQAM/UFMC/NOMA.

Parameter	Characteristic
FFT size	1024
Sub-band offset filter	156
Sub-band size	24
Type of MAPF filter	Dolph Chebyshev
Filter length	64
Modulation	4, 16, 64, and 256 OQAM
Sub-carrier mapping	Localization
Bits per subcarrier	1, 2, 4, 8
Frequency	16 MHz
Bandwidth of AWGN channel	24 MHz

4.2 Practical considerations

For numerous reasons, such as temporal synchronization between transmitting and receiving, the frame length in most linear applications must be set. As a result, the duration of a temporal frame T is considered to be fixed throughout this work. However, depending on the number of samples obtained by an SU and the number of SU in CSS, the sensing or reporting length within a given time frame may be varied. The longer the detection period, the more samples are gathered for detection. Likewise, the greater the reporting time will be, the more SU that engage in CSS and/or the bigger the number of packets used for transmission. It is worth noting that greater detecting and sending times result in lower data transmission which contributes to a lower spectrum utilization likelihood. As a result, there is an intriguing trade-off to be made between the number of SU and sending bits versus spectrum usage. It is worth noting that there is a chance that SU will use the idle frequency band during the communication slot of a particular time frame before PU reappears in that spectrum band. For SU, spectrum efficiency is primarily determined by the accuracy with which the removal of the primary signal is detected and the duration of data transmission. The greater the correct detection likelihood and the greater the transmit duration, the more spectrum is predicted to be used.

4.3 Optimal utilization of cooperative spectrum sensing

While the ideal number of SU is predetermined, the optimal number of bits for reporting can still be achieved. A resource allocation plan that takes into account the user variety of SU in channel state, traffic load, and energy amount is proposed to maximize the long-term network-level throughput in energy-constrained cooperative cognitive radio networks (CCRN). For each SU to experience the same SNR of the sensing channel in the primary signal's coverage region, it is assumed that each SU is Independently and Identically Distributed (IID). Due to its straightforward implementation and lack of requirement for prior knowledge of source signal and channel fading, an ED technique is assumed for spectrum sensing.

During the sensing phase, each SU gathers S observations from the channel and communicates the energy value of those observations to the FC in the form of a quantized representation of N. When the FC receives the quantized energy value from all SU, it integrates them and analyzes them to a predefined threshold level (λ) to conclude. Employing the conditional probability theorem to several samples and users yields the Detection Probability (DP) and false alarm probability FA (PFA) given in Eqs. (8) and (9).

$$\mathrm{PFA} = \begin{cases} Q^{\lambda}\sigma^2 - 1; \\ 0, \quad \sigma^2 \end{cases} \tag{8}$$

$$\mathrm{DP} = \Pr(\mathrm{Energy} > \lambda | H_1|) = Q, \lambda - \gamma - 1 \times \mathrm{MS} \tag{9}$$

where MS represents the time in milliseconds. γ is SNR and Q is Q-function. Due to performance constraints, a specific degree of detection probability is frequently required in actual systems. When given a target detection probability, the detection threshold may be determined using Eq. (10).

$$\lambda t = \sigma^2 \lambda + r^2 \lambda + 1(Q-1) \times (\mathrm{DP}) \tag{10}$$

The likelihood of a false alarm may be recast as a proportion of objective detection probability by substituting Eq. (10) into Eq. (8).

$$\mathrm{PFA} = Q\sqrt{2} \times \gamma + C(Q-1)(\mathrm{DP}) + \gamma \times \sqrt{\mathrm{MS}} \tag{11}$$

PFA computed at FC falls as the number of SU increases in soft CSS. PFA is affected by the number$N$ utilized in data sending to FC. PFA decreases as N grows because as the quantity of reporting bits improves, so does the number of quantization levels ($2N$), which aids in achieving low PFA. As a result, having a low PFA increases the probability of accurate detection (P_{cor}) of primary users' signals, allowing SU to better use unused spectrum bands. Communication of SU is deemed successful if it occurs during the PU idle time, which needs the PU idle time to be longer than SU data transmission, in other words, there is no PU appearance in the spectral during SU data

transmission (T_r). This prevents secondary users from interfering with the principal user.

Forming a network of cognitive radio users, choosing appropriate sensing methods, designing an effective cooperative protocol, ensuring synchronization, allocating channels for sensing, developing effective data fusion algorithms, making precise decisions for spectrum access, incorporating a feedback mechanism, continuously adjusting and optimizing the system, and regularly evaluating its performance are all necessary to achieve the best possible utilization of cooperative spectrum sensing. These procedures facilitate cooperation, precise sensing, trustworthy decision-making, and adaptive optimization, which leads to effective spectrum utilization and enhanced overall performance of the cooperative spectrum sensing system.

4.4 Cognitive radio network using OQAM/UFMC/NOMA for Internet of Things

One of the primary challenges faced by UFMC developers is the large level of PAPR. Furthermore, recent research may be combined the metric with the PAPR to demonstrate the signal's energy back-off impact, in which the PAPR measure detects the highest peak while the quadratic metric detects the Out of Band leakage and In-Band deformation[29, 30]. The majority of existing methods, such as intensity clipping, tone reserve, and active constellations expansion, reduce PAPR while lowering the bit error rate[31, 32]. Selected shifting is a promising approach that has lately been utilized to tackle the PAPR and CM issues without degrading the Bit Error Rate (BER). The EEAPF is used in conjunction with UFMC to minimize PAPR while maintaining BER in 5G networks. Because of the consistency of sub-carriers in the spatial domain, multicarrier transmission schemes have a high PAPR. High PAPR causes the power amplifier to enter the nonlinearity zone, resulting in out-of-band emission, IB distortions, and lengthy word length. The digital-to-analogue converter's large word length is a critical issue that drastically decreases battery life. To eliminate the PAPR in the waveform, many methods are offered. The EEAPF technique is used to eliminate PAPR.

The problem of a high PAPR, which frequently occurs in multicarrier systems, is addressed in our suggested methodology for CRN using NOMA. We use methods like Selected Mapping (SLM) or Partial Transmit Sequence (PTS) to lower the PAPR to get rid of this problem. To reduce the strong PAPR effects, these methods include changing the broadcast signal in the time or frequency domain. By utilizing these strategies for PAPR reduction, we make sure that the transmission in our CRN employing NOMA maintains a low PAPR, preventing bit-error rate deterioration and improving system performance as a whole.

In 5G, UFMC is a new QAM-type multicarrier modulation that may be used instead of NOMA and FBMC waveforms. In contrast to FBMC, which uses self-subcarrier modulation, UFMC uses a group of subcarrier modulation. When compared to FBMC, subcarrier grouping reduces the length of the filter while also reducing the performance time. UFMC may be thought of as a generalized variant of the NOMA, starting with the standard OFDM system.

The following are some ways that NOMA-UFMC is used to improve CSS. First, NOMA-UFMC uses cutting-edge multi-user interference cancellation techniques to allow numerous users to share the same frequency and temporal resources. As a result, the spectrum can be used more effectively and with better spectral efficiency. Additionally, because it makes use of filter banks that can reduce inter-symbol interference, NOMA-UFMC offers robustness against fading channels. Cooperative users can execute simultaneous sensing and communication by integrating NOMA-UFMC into CSS, which improves CSS in cognitive radio networks by boosting overall spectrum sensing performance and enhancing sensing accuracy.

Let NOMA be written as in Eq. (12).

$$X(\mathrm{e}^{\mathrm{j}\Omega}) = \sum_{n=-\infty}^{\infty} X[n]\mathrm{e}^{-\mathrm{j}n\Omega} \tag{12}$$

where

$$\Omega = \frac{\omega}{f_s} = \omega T.$$

Here, X set is created using OQAM modelling, where X is the NOMA transmissions that indicate an Inverse Fast Fourier Transform (IFFT) of standard size NFFT, k is denoted as time index, and n is the wavelength guide, respectively. Completely identical independent distribution makes up the X set. Equation (12) has a constructively or destructively compounding. As a result of information coherence aggregation, there will

be a big peak relative to the average, which is known as PAPR. The NOMA (cyclic-prefix free) used in LTE may be created by applying the filter over the whole band, as shown in Eq. (12). The NOMA is obtained by using the filter in Eq. (13).

$$y = U \times V \tag{13}$$

where NFFT can be written as the number of transmission subcarriers at the transmitter end and U is the IFFT vector of size N. As a result, Eq. (14) is

$$X(\mathrm{e}^{\mathrm{j}n\Omega}) = \left(\frac{1}{t}\right) X_a(\mathrm{j}nwT), -\pi < \Omega = \omega T < \pi \tag{14}$$

where n is in the range of $[0, \mathrm{NFFT}-1]$. The UFMC scheme may be specified as an equation if the full band is segmented into R sub-bands as in Formula (15).

$$y \sum_{i=1}^{R} G_r \times U_r \times V_r \tag{15}$$

where G is the Toeplitz vector NOMA transmission at the end of the transmitter of the Finite Impulse Response (FIR) filter, which achieves the direct alteration across the band of N. The final windowed data sequence is

$$\{\ldots, 0, y[0], y[1], \ldots, y[\mathrm{NFFT}-1], 0, \ldots\} \tag{16}$$

Using the finite sequence as given below,

$$\{y[0], y[1], \ldots, y[\mathrm{NFFT}-1]\} \tag{17}$$

denoted by

$$\{y[\mathrm{NFFT}]\}, N-1 \tag{18}$$

The OQAM signal elements of V_r are first translated to the spatial domain using the relevant entry of the IDFT vector U_r, which correlates to the given sub-band r inside the frequency spectrum, in Formula (15). G_r is the sub-band filter that corresponds. The whole UFMC system is obtained from Formula (15). To accomplish two times up-sampling, the procedure starts with zero padding at the receiver end. The carrier frequencies (down-sampling) of a junction are then picked using the 2N-DFT until the OQAM de-mapping is used to gather the collected signal.

The architecture of OQAM/UFMC/NOMA is shown in Fig. 4 and shows how the filtering process uses a block-wise variant of Physical Resource Block (PRB) to increase the architecture's adaptability. The filter length, $P >> 1$, and X all include one OQAM signal, therefore they play an important part in the system's construction. The spatial domain characteristics may be smaller (on the choice of cyclic prefix period of usual CP-NOMA, allowing the system to support Transmits Short Messages) as the bandwidth filter length is long. Furthermore, unlike the FBMC signal architecture, side-lobe removal occurs at the endpoints of the sub-bands rather than between the subcarriers. The time-domain stepping up/down provides more barriers against the occurrence of Inter-Symbol Interference (ISI) that could be eliminated by CP. The FBMC characteristics are dissimilar from the UFMC that maintains complex orthogonality, allowing the UFMC to effectively communicate the MIMO method for multiple users. The UFMC, on the other hand, is more productive than NOMA in terms of spectrum build since it lacks a cyclic prefix. The procedure begins at zero paddings on the receiving end to produce a two-fold up-sampling. After that, UFMC may achieve OQAM de-mapping to gather the received data by performing the 2N-DFT and choosing every other subcarrier, which is down-sampling, as illustrated in Fig. 4.

4.5 Accurate data gathering for IoT CRN 5G wireless communication

There are three types of IoT data gathering:

(1) **Equipment data**. This type of data pertains to the state of IoT devices. Equipment data is collected in real-time to allow predictive maintenance tasks. Predictive Maintenance does not have to be the sole realm of Data Scientists. Check out this video to discover how to apply machine learning for PdM. In buildings where several tenants utilize utilities like water, electricity, gas, or cable, submeter data can be gathered. Digital measuring equipment minimizes measurement costs, mistakes, and billing timeliness.

(2) **Environment information**. Environmental data may be measured and monitored by IoT devices. These data streams are used to track physical labour conditions to minimize disasters such as flooding and air toxicity. As a result, it saves the system a significant amount of energy while increasing machine productivity and lifetime. To make equipment data more helpful, it should be consolidated and accessible to line employees, tactical management, and senior executives.

(3) **Submeter information**. Submetering enables property owners to automate the measurement of individual utility use in multi-user environments.

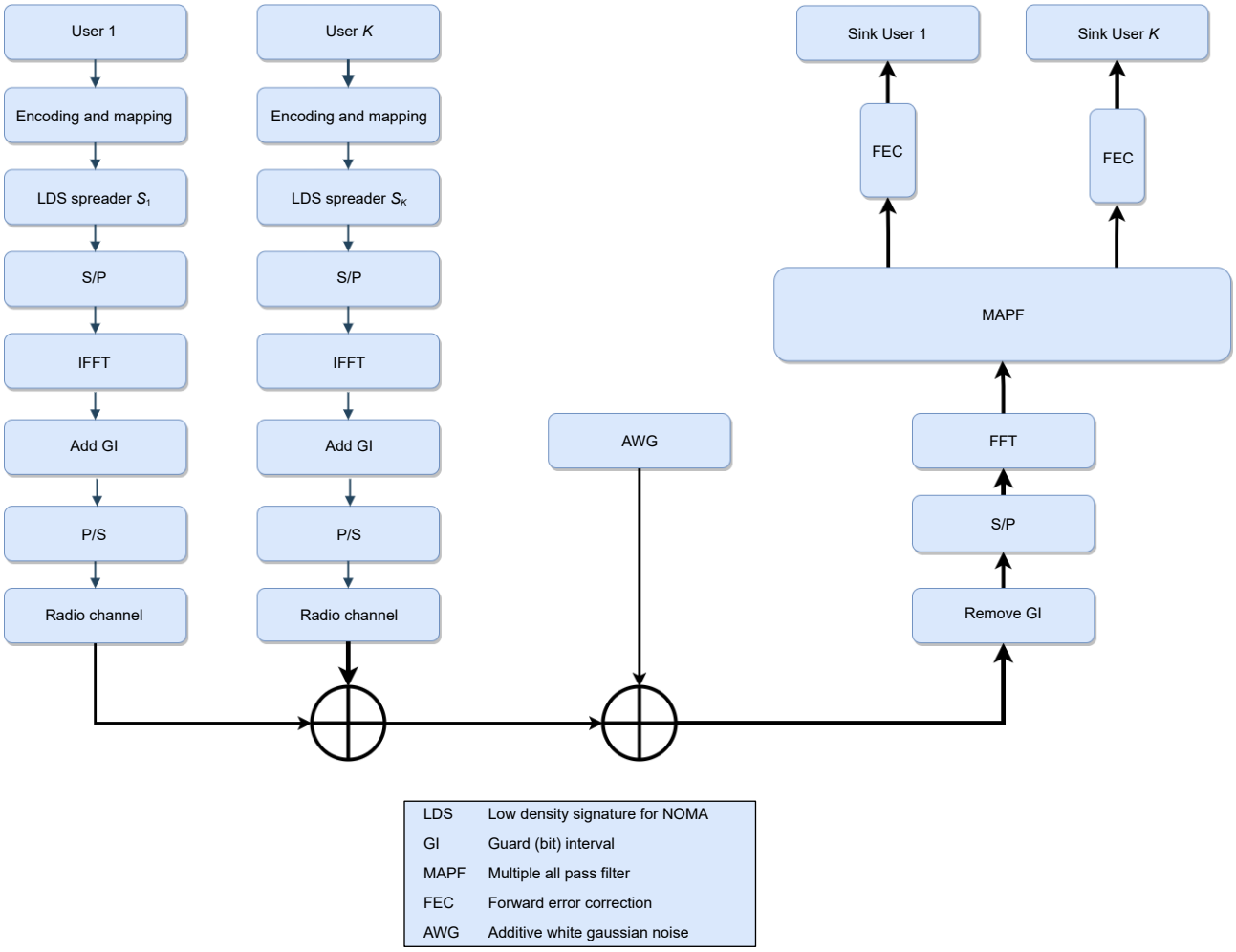

Fig. 4 Proposed architecture diagram of OQAM/UFMC/NOMA for IoT.

A novel architecture could be established to improve the underlying part of a WSN CRN with CR functionality for accurate sensors' energy monitoring, energy-consuming stream hand-off removal, an effective energy brokerage and service quality availability of data transfer rate to the sensing device application areas through CRN network. The large WSN is grouped into regions for energy consumption, with each group connected to a surface central processor. For optimal spectrum usage, the protocol contains an optimal recurrent learning method, which enables data collection from devices while simultaneously addressing environmental concerns. WSN predicts PU traffic and adapts to spectrum and intervening situations on a per-flow basis to prevent clashing with licensed users.

The proposed methodology focuses on long-term alternatives for sensor nodes to gather sensor data while using CRN capabilities and taking into consideration the needs of the sensors' operations, centralized, group, and decentralized radio resource management methods are three types of radio resource management techniques. In the centralized system, all of the sensors communicate directly with the base station or sink node, allowing for higher data transmission and locally optimal responses. This approach becomes inconsistent with disruption procedures as the data collection period increases. When the mobile network grows, a group strategy is chosen since it allows for more mobility and community resource distributions, which means that detecting updates does not have to be transmitted to the central and connectivity capacity does not have to be divided among all of the network's devices. Signalling is decreased as the number of sensor nodes in the group decreases, and the sensors may transmit at lower power.

The dispersed method does not give the most cost-

effective capacity planning. A CRN WSN is made up of clusters of devices. The CRN feature offers plug-and-play compatibility for a variety of network-based applications. This is accomplished through the directly attributed plane, which allows for a wide range of data transmission rules, and the application layer, which combines higher activities from access points (sensor network) and provides operations with a global view of the network elements. Flows are the appropriate software data flow through the CRN framework. Improvements to the CRN lower layers features, namely medium connectivity, are recommended so that aspects such as sustainability and QoS configuration management in terms of data frequency flow, as well as effective energy brokering with dynamic channel access assessment tasks to avoid channel access threats, are possible.

The Cluster Head (CH), which supports the network devices that are fully accountable for information-related functions, is a node that enables the data plane in each group. An inter-domain link connects the CH to the other CHs and the sink. The cluster's traffic is finally routed to the SN, which link to the computing main controller.

Clustering has increased energy efficiency through the selection of cluster heads, but its implementation is still challenging. The sites where cluster heads are desired are initially explored via the existing cluster-head selection methods. The cluster heads are then chosen from the nodes that are most nearby these points. Seven phases make up the energy efficiency exploration: initialization, local leader, global leader, local leader learning, global leader learning, local leader decision, and global leader decision phases. In contrast to a typical method, an exploration sample-based method updates the exploration samples and location at the same time.

The most prevalent issues encountered are network holes and isolated nodes. In a multihop environment, the CH near the base station consumes energy more quickly than the nodes far from the base station due to the network hole problem, also known as the hot-spot problem, where the majority of data is transferred to the CH near the base station for aggregation and data transfer to the base station. The isolated node problem, on the other hand, occurs when nodes do not join any cluster and do not have a way to convey data to the base station.

The Cluster Head (CH), which implements the control plane in CRN WSN, sends communication to the sink node through secure channels. The CRN WSN is regarded as large enough to justify its split into clusters. The clusters are arranged locally, reducing the amount of power required since broadcasting to the CH uses fewer resources than transmitting immediately to the sink node, increasing the cluster's lifetime and allowing spectrum recycling. Intra-cluster information is transmitted over a communication link that is chosen so that the control channels of nearby clusters do not conflict. Sensor nodes, also known as cluster heads or core networks, are useful for interacting between adjacent clusters. The CH calculates the SNR of its streams, and if the SNR falls below a specific level, the network is removed from the list of CR communications aspiring to be streams. For the CH to select the best available channel as the control channel, it employs an optimum supervised learning scheme to learn about PU traffic and identify the greatest distribution possibilities, i.e., those that are not disrupted by PU arrival. By providing their SNR values, the sensors help this process. Even though the cluster is tiny and the SNR circumstances inside it tend to be similar, there may be outliers, and the sensors can transmit their SNR state to the CH. CH is chosen from many other strong sink nodes and is in charge of cluster maintenance as well as cluster security. The CH also gathers the sensors' data rate needs for their streams and sends them to the sink for improvement. Because the CH are unable to perform high research techniques, those jobs are sent to the SN and the cloud. The cluster accepts the flow data rates after obtaining the optimization findings, and the sensors change their transmitting power and data rate appropriately. Communication between SU and PU is shown in Fig. 5.

The algorithm is developed for sensor node activities concerning CH.

Algorithm 1 involves initializing variables and parameters related to data transmission, signal-to-noise ratio, modulation type, waveform type, and latency. The algorithm then loops through iterations to estimate the delay, estimate the spectrum at the primary user, and transmit the data. The sleep state is entered at the end of each iteration.

Algorithm 2 involves generating random input data and transforming it using OQPSK modulation. The algorithm also calculates the SNR and best Eb/No

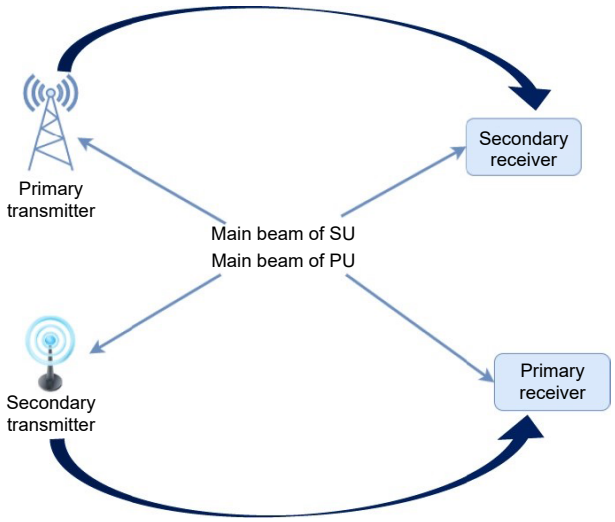

Fig. 5 Communication between SU and PU.

Algorithm 1 Start mobility of data at sensor node

Begin
Data = 1×10^6 bits
eps = 1×10^{-4}
Datasize = 10 000; spectrum and initiates supervised learning
SNR = 0 : 2 : 40
SNRindB=$10^{(SNR/10)}$
Modulation_Type = OQAM
5GW = UFMC
Initialize $D_i = D_j$ = AE
for k = 1, k_n, k++ do
  for Iteration = 1 : end
    Power = eps×SNRindB(Iteration)
    Hmatrix = Latency minimize
    $q \leftarrow 0$
    eps $\leftarrow 1\times10^{-6}$
    $i \leftarrow 0$
    Convergence ← false
    Estimate delay using XOR vector
    Estimate spectrum at PU and convey the data
    Go into a sleep state
  end for
end for
End

values for the transmitted signal. The algorithm then loops through iterations to transmit the 00000000 message to the primary device, receive data at the network layer, and select U_1 and U_2 based on minimum and maximum functions.

Algorithm 3 is concerned with the efficient reception

Algorithm 2 Start mobility of data at cluster head

Begin
Bits = 1×10^4
Input = rand(1, Bits) > 0.5
Ortho = 2 × Input − 1
Distance = 1 : 20
Energy = 25
SNRindB = Energy + $10\times\log_{10}$(Subcarrier) + $10\times\log_{10}$(64/80)
Best Eb/No in decibels
00000000[Datasize] is sent to the main processor
for j = 1, j_h, j++ **do**
  if $T_j > d$ **then**
    Primary device's 00000000[Datasize].
    N/*W* layer receives data
    U_1 = fargmin(W_i)$g[U_1]$
    U_2 = fargmax(W_i)$g[U_2]$
  end if
end for
End

and processing of data in a CRN context, with a focus on spectrum estimation and classification, channel estimation, and signal processing techniques. The main phase data receiver CRN OQAM WSN is derived from Algorithm 3. The count of the samples is supplied as $N = 1\times10^6$ with the input values with the transmitter data, the Eb/No is initialized to [0 : 25], the transmitter and receiver have 2 channels, and the error is equal to WSN CRN SNR; the initialization of scaling parameter S, f, Q, with N subcarrier, and $T-$Th segmentation. For the j^{th} subcarrier signal, the spectrum estimate is performed. The calculated signal is normalized. The j^{th} segment is considered if the normalized signal is bigger than the segmented signal. CRN with spectral efficiency fresh data and CSS yields the highest throughput. Furthermore, n values are used to calculate the number of users.

4.6 Experimental setup

The MATLAB 2022 is used for research and development. The following is a full list of the probabilities utilized in the research and the experimental environment. These will also be utilized to obtain a simulation model, which will validate that the practical application is correct:

(1) PPS is denoted as the probability of successful transmission among the primary user transmitter and secondary user transmitter.

Algorithm 3 Main phase data receiver CRN OQAM WSN

Begin
$N = 1 \times 10^6$
Eb/No = [0 : 25]
$n_{Tx} = 2$
$n_{Rx} = 2$
WSN_CRN_SNR = Error/N
CRN_SNR = $0.5 \times \text{erfc}(\text{sqrt}(10^{(\text{Eb/No}/10)}))$
$\text{Eb/No} = 10^{(\text{Eb/No}/10)}$
Sensor spectrum ensemble classification
Initialize $S, f, Q, n_{sub}, \text{Th}_{seg}$;
Spectrum estimation
for $(j - n_{sub})$ **do**
  Compute $Y_{j\text{norm}}$
  if $(Y_{j\text{norm}} > \text{Th}_{seg})$
    Consider j^{th} as segment1
    then count ++;
  end if
  total_segment = n_{sub} + count + 1
  Starts sending the updated 00000000[Datasize]
  Primary processor if the 00000000[Datasize]
  Maximum throughput
  Spectral efficiency new data 00000000[Datasize] and CSS
end for
for $(j - \text{total\_data})$ **do**
  number_users = n
  $\text{SU}_{ij} = \text{SU}_{ij1}, \text{SU}_{ij2}, \text{SU}_{ijn}$;
end for
for $(r - n)$ **do**
  Classify signal as low SNR or high SNR; If (SNR==low)
  MFD is used;
  Compute EST2;
end for
End

(2) PSD is denoted as the probability of successful transmission among the secondary user transmitter and primary user receiver.

(3) PPD is denoted as the probability of successful transmission among the primary user transmitter and primary user receiver.

4.7 Assumptions

Suppose that PPS and PSD are larger than PPD to optimize the results of cooperation cognitive transmitting. This means that the communication channel between PU_{Tx} and PU_{Rx} through SU is comparably larger than the data transmission among PU_{Tx} and PU_{Rx} immediately. For cooperate cognitive transmission, this is the optimal circumstance. In other words, the possibilities are set to values that will simulate the channel condition, and they are set to values that will replicate a better channel circumstance between PU_{Tx}, and SU_{Tx}, SU_{Tx}, and PU_{Rx} than PU_{Tx} and PU_{Rx}. As a result, PPS = 0.95, PSD = 0.95, and PPD = 0.70 are considered.

5 Result and Discussion

In this section, the test results of the proposed methodology are presented and discussed. Our experimental analysis performs simulations to validate the performance of the proposed methodology and discusses the results. The experimental parameters are listed in Table 1. Table 1 details the many characteristics employed in calculations and analyses. FFT size is 512, with 10 sub-bands and 20 sub-carriers, as shown in Table 1. One of the most significant factors to assess system performance is Cubic-Metric (CM) or PAPR evaluation. PAPR analysis was chosen over CM analysis because it is frequently used in research to examine multicarrier signals.

At the transmitter, complex signals are produced using OQAM for WSN communication systems. The additional DC bias, however, cannot completely prevent zero clipping when taking into account the peak power restriction. In the meanwhile, the DC addition may result in peak power clipping distortion. The DC bias needs to be eliminated at the receiver before the *M*-QAM data can be retrieved and demodulated in WSN.

Table 2 summarizes the CCDF analysis of the PAPR evaluation using 4 OQAM, 16 OQAM, 64 OQAM, and 256 OQAM, correspondingly, at a clip rate of 1×10^{-3}. Table 2 shows that raising the magnitude in MPAF, which is a power allocation factor, causes the PAPR of the UFMC signal to drop, at the revalued amount of the system's functionality. The performance of current wireless communication is significantly improved by NOMA-UFMC and cooperative SS based on modulation. One of the techniques that are better suited for deployment in 5G communication systems is NOMA-UFMC. NOMA-UFMC works on system modulation to establish user orthogonality. It is a really simple solution that not only makes the system more efficient overall but also makes it simpler. Real and distant users are modified separately on the

Table 2 OQAM comparison for multi-carrier waveform generation.

Multi-carrier waveform	4 OQAM	16 OQAM	64 OQAM	256 OQAM
OQAM/UFMC/NOMA	12	12	12	12
UFMC/NOMA	7.4	7.5	8	8.5
UFMC	7.2	7.3	7.8	7.9
OQAM/OFDM	7.1	7.2	7.4	7.6

constellation of the modulation in NOMA-UFMC by the BS. Near users are modulated on the real component of the OQAM constellation, and far users are modulated on the imaginary components. In terms of a smaller number of SICs, NOMA-UFMC lowers the symbol error rate, inter-cell and inter-cluster interference, latency, and computational complexity. The PAPR decrease is also influenced by the variation size. When relative to the NOMA-UFMC pattern, the influence of incorporating diverse QAMs is more evident on the GCL pre-coded UFMC waveform and MPAF channel estimation UFMC waveform with $V = 2, 4, 16,$ respectively. With higher cognitive modulations, PAPR performance decreases. As a result, the modulating size should be carefully chosen for 5G wireless IoT.

The proposed approach offers a fresh method for lowering the PAPR through filtering. The findings revealed a notable decline in PAPR with an average drop of 32.8%, without impairing BER performance. The suggested method takes significantly more computing power than the prior methods, according to the computation complexity study. This is mostly due to the simultaneous execution of IFFTs, phase searching, and candidate selection at both the real and imaginary sections. Also, the suggested method's BER performance with the effect added demonstrates improvement with a 25% decrease in the BER with 256 OQAM.

Figure 6 shows a simulation of CRN for 5G wireless communication using OQAM/UFMC/NOMA. In both the absence and presence of the primary user, a CR network is proposed to allow a secondary network comprising SU who want to access the 5G spectrum. In particular, SU can use the OQAM/UFMC/NOMA method to connect with two destinations, which can significantly increase spectrum usage when compared to the NOMA schemes for 5G wireless IoT. The colours of the lines in both Figs. 7 and 8 represent an interactive display of the different subcarriers to show the difference between them. Figure 7 shows CRN synchronization for a reliable cooperative spectrum.

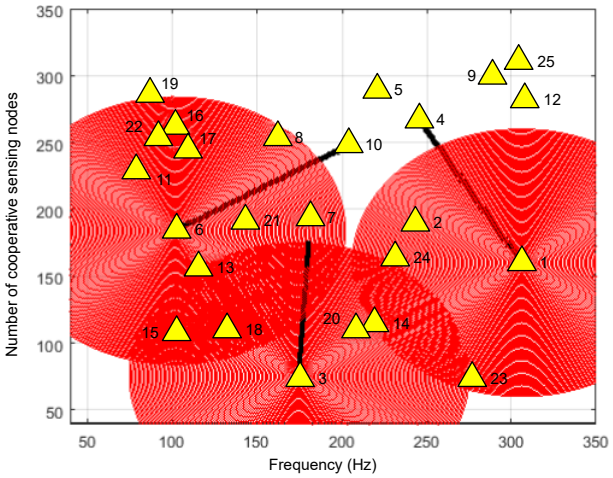

Fig. 6 Simulation of CRN for 5G wireless communication IoT.

For maximum synchronization, appropriate beamforming between antennas is used. For computing maximal norms and vector projections, a channel matrix was created. The technique is continued until the smallest associated antenna is found. Even though the system's computing complexity has been reduced, it still fails to improve performance.

Figure 8 shows CRN's reliable limited cooperative spectrum. Soft Choice Scheme, in which the CRN collects and combines the test statistics generated at the SU to compare a final test statistic to a limit and

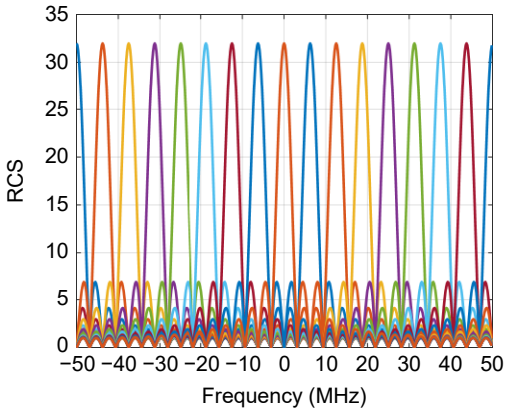

Fig. 7 CRN synchronization for reliable cooperative spectrum (RCS) IoT.

determine a primary channel selection. This section displays the performance improvement as a function of the reliability factor. In Fig. 8, the BER of channels is changed, and the normalized average reliability values of control channels selected using current methods and the soft choice scheme are presented. The reliability factor is weighted in the utility function to ensure the selection of highly reliable channels with a low error rate. According to the reliability study, the soft choice scheme picks the channel with the lowest BER readings and offers an improved environment amid noisy settings. Figure 9 shows the relationship between SNR and PD for 5G wireless communication for 5G wireless IoT. When the average SNR of sensing node 1 changes from −20 dB to −10 dB and that of sensing node 2 is set at −15 dB, the detection performance for a single and two data aggregation scenarios is compared. For the equal thresholds scenario, it can be seen that the average SNR's effective range is rather limited for 5G wireless IoT.

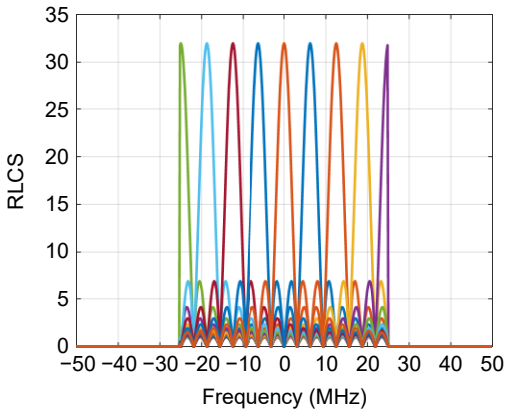

Fig. 8 CRN reliable limited cooperative spectrum (RLCS) for 5G wireless communication IoT.

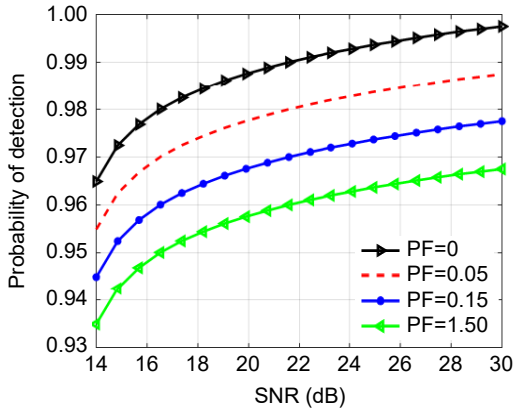

Fig. 9 Relationship between SNR and PD for 5G wireless communication IoT.

Figure 10 shows capacity maximization for different modulation schemes for CRN 5G wireless communication. The simulation system is set up to check the effectiveness of the classification approach in terms of energy consumption, interference produced by the secondary system to the PU linkages system, and its user capacity. Between the transceivers, two pairs of PU connections with a distance of 10 m are formed. Each node in the CRN system is expected to have synchronization antennae. When the SNR increases, the capacity in Mbps also increases. The latency is reduced due to an increase in capacity. If the SNR in dB is increased, the capacity in Mbps is also increased. The SNR and capacity are linear and propositional to each other. The latency ID is highly reduced due to an increase in the capacity and SNR. The capacity of the proposed methodology is higher than other methodologies. The proposed methodology has high SNR in dB as it reached 37 Mbps. The other methodologies' capacities are reduced considerably. Figure 11 shows CRN 5G Link quality Receiver Operating Characteristic (ROC) curve. In two different circumstances, the suggested approach is compared to energy detection: AWGN channel and Rayleigh channel. The algorithms' performance is measured using ROC curves, the PFA, and the PD over a range of SNR values.

The latency of CRN NOMA for 5G wireless communication is highly reduced as shown in Fig. 12. The OQAM/UFMC/NOMA reached 0.01 latency error and it reached 40 dB SNR, thus the variation of error varies from 0.01 to 0 for obtaining 40 dB. Other methodologies take high latency errors to reach 40 dB. The UFMC/NOMA has reached a higher error of 0.04

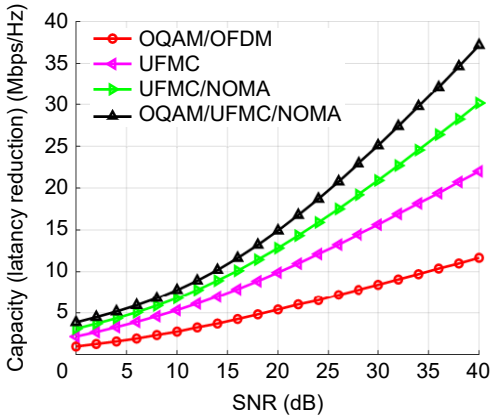

Fig. 10 Capacity maximization for different modulation schemes for CRN 5G wireless communication.

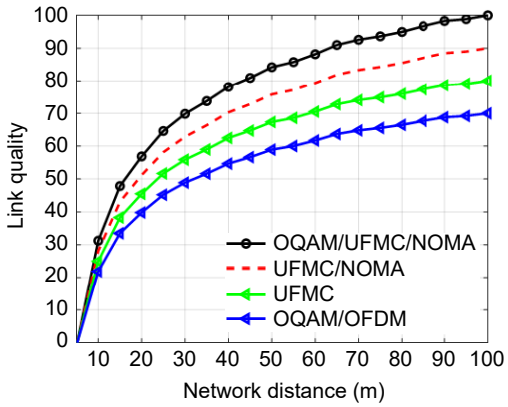

Fig. 11 CRN 5G Link quality ROC curve.

for SNR in 40 dB. The UFMC has reached a higher error of 0.05 for SNR in 40 dB. The OQAM/OFDM has reached the highest error of 0.08 for SNR in 40 dB.

For CRN, Fig. 12 depicts the estimated one-hop latency minimization of various SU nodes. CRN has the shortest transmission delay when compared to the other techniques for proving latency minimization. As a result, the proposed method provides reduced transmission delay and near-optimal power usage for each SU node in the network. Figure 13 shows PAPR reduction using EEAPF for CRN 5G wireless communication IoT. For N = 64 and N = 256, the proposed technique is used. With 10.7 dB and 11.3 dB at a probability of 1×10^{-3}, correspondingly, the PAPR of the pure OQAM/UFMC/NOMA signal is the greatest. The EEAPF for CRN 5G is proposed for minimization PAPR for OQAM/UFMC/NOMA. IFFT are used by the EFFAPF filter to create several waveform candidates. The waveform candidate with the lowest PAPR is chosen to transmit the OFDM symbol. The OQAM/UFMC/NOMA has achieved low

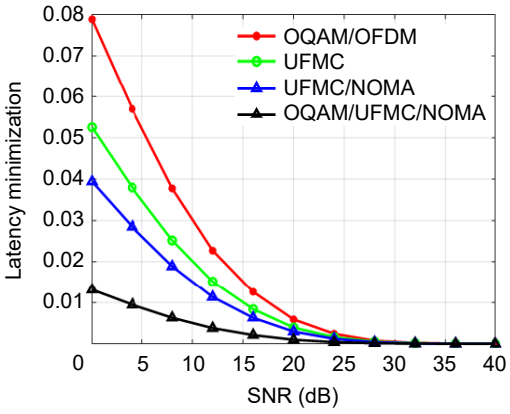

Fig. 12 Latency minimization for CRN IoT 5G wireless communication.

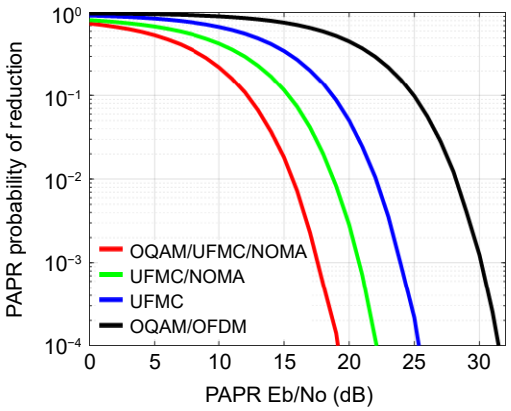

Fig. 13 PAPR reduction using EEAPF for CRN IoT 5G wireless communication.

PAPR and reached high SNR in 30 dB. The UFMC has achieved a low PAPR and reached high SNR in 25 dB. The UFMC/NOMA has achieved low PAPR and reached high SNR in 22 dB. The OQAM/OFDM has achieved low PAPR and reached high SNR in 18 dB.

Figure 14 shows Carrier Frequency Offset (CFO) synchronization error minimization for CRN 5G IoT. Because of its homogenous distribution features, high spectral efficiency, and low carrier frequency offset, OQAM is frequently employed in 5G communication. Figure 15 shows Symbol Error Rate (SER) minimization for M-OQAM/UFMC/NOMA. The various OQAM M-array modulation techniques are applied to minimize SER to improve the CSS of OQAM/UFMC/NOMA. The OQAM/UFMC/NOMA obtained minimized error of 0.04 and high SNR of 35 dB. The UFMC/NOMA obtained a high CFO mismatch error of 0.08 and reaches high SNR in 35 dB. The UFMC has reached a high CFO mismatch error of 0.12 and reached high SNR in 35 dB. The OQAM/OFDM obtained a high CFO mismatch error of 0.13 and reaches high SNR in 35 dB.

Figure 16 shows throughput maximization. The proposed OQAM/UFMC/NOMA methodology provides better throughput when compared to other methodologies. The OQAM/UFMC/NOMA reaches around 98% of throughput in the performance. The other UFMC/NOMA, UFMC and OQAM/OFDM are lesser performance than OQAM/UFMC/NOMA. The improved SNR minimized BER, minimized PAPR, minimized CFO and minimized latency is used to provide better throughput maximization as shown in the graph. To maximize the throughput of NOMA-based 5G networks, the study gives a thorough review

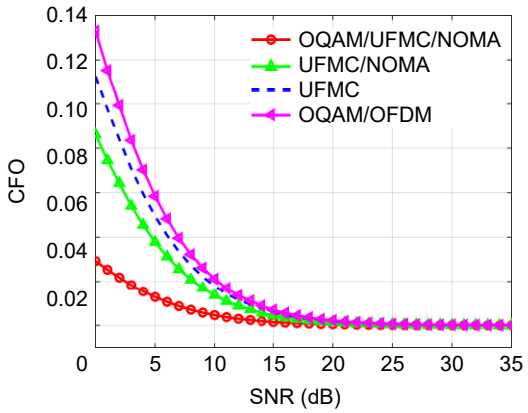

Fig. 14 CFO synchronization Error minimization for CRN IoT 5G.

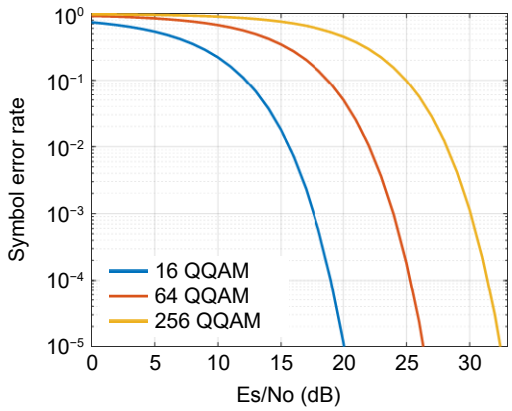

Fig. 15 SER for M-OQAM/UFMC/NOMA.

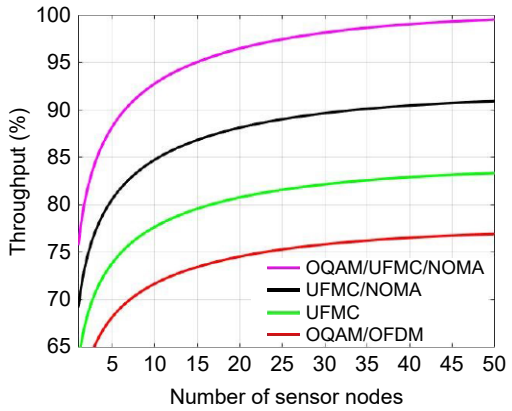

Fig. 16 Throughput maximization.

of the throughput performance in power allocation systems. It describes the principle of the NOMA-based system and offers an example of throughput computation. The paper also addresses the power allocation issue formulation in terms of the algorithms used, goal functions, restrictions, problem limits, and considerations. Moreover, the article compares existing water-filling algorithms to the improved methods in terms of throughput performance, time efficiency, and computational complexity. Finally, the channel state is a crucial signal for power allocation. Methods for improving network performance may include increasing the number of multiplexed users on the same subcarrier.

The performance of the system is significantly impacted by the proposed methodology's mitigation of CFO synchronization error. A CFO synchronization issue can result in frequency misalignment between the transmitting and receiving nodes, which can impair system performance and cause Inter-Carrier Interference (ICI). The suggested methodology enables precise frequency alignment, lowering ICI, and enhancing signal quality by minimizing CFO synchronization error. As a result, BER are reduced and detection accuracy is improved. Furthermore, reduced CFO synchronization error enables improved spectrum utilization, boosting spectral efficiency and total system capacity. By reducing the effects of CFO synchronization problems, the suggested methodology benefits from increased system dependability and performance.

6 Conclusion

This research offers a multi-carrier waveform for cognitive radio networks in 5G wireless communication. To evaluate the PAPR performance of the proposed waveform, simulations were run in MATLAB. In this study, the EEAPF is used to increase the PAPR gain utilizing the OQAM/UFMC/NOMA technique. The results of the computer simulations demonstrate that the suggested waveform produces superior PAPR results than conventional NOMA-UFMC signals, i.e., at a clip rate of 1×10^{-3}, the suggested waveform produces about 4 dB of PAPR gain when compared to standard NOMA-UFMC waveform employing OQAM. It is worth noting that the proposed methodology has a somewhat high level of design complexity. However, the suggested waveform's complexity can be reduced by employing smaller FFTs and lowering the number of sub-bands. The suggested waveform has a substantial advantage over existing waveforms in terms of capacity and PAPR reduction. In compared to existing waveforms, the suggested waveform has a large capacity. Optimal

CSS for CRN is performed using OQAM/UFMC/ NOMA methodologies. The availability of spectrum and bandwidth utilization are key challenges in CRN for IoT 5G wireless communication. To show the benefits of the proposed approach, we investigate three cases: complete tracking (pilot-aided tracking + effective channel gain update), limited tracking, and no tracking. Specifically for the complete tracking situation, performance comparisons are done between different OFDM receivers utilizing the three techniques to demonstrate the BER improvement of the proposed recursive estimating algorithms. The BER performance of an offset-free OFDM system with perfect channel information is also simulated for comparison with systems using a full, partial, or no error tracking approach. The optimal solution should be given for CRN for IoT-based 5G communication to provide optimal bandwidth and CSS, low latency, SNR improvement, maximum capacity, offset synchronization, and PAPR reduction.

References

[1] A. Nasser, H. Al Haj Hassan, J. Abou Chaaya, A. Mansour, and K. C. Yao, Spectrum sensing for cognitive radio: Recent advances and future challenge, *Sensors*, vol. 21, no. 7, p. 2408, 2021.

[2] H. Wu, D. Mo, and H. Li, Analysis and simulation of the dynamic spectrum allocation based on parallel immune optimization in cognitive wireless networks, *Sci. World J.*, vol. 2014, p. 623670, 2014.

[3] W. Lee, M. Kim, and D. H. Cho, Deep cooperative sensing: Cooperative spectrum sensing based on convolutional neural networks, *IEEE Trans. Veh. Technol.*, vol. 68, no. 3, pp. 3005–3009, 2019.

[4] J. Feng, M. Zhang, Y. Xiao, and H. Yue, Securing cooperative spectrum sensing against collusive SSDF attack using XOR distance analysis in cognitive radio networks, *Sensors*, vol. 18, p. 370, 2018.

[5] F. Awin, N. Salout, and E. Abdel-Raheem, Combined fusion rules in cognitive radio networks using different threshold strategies, *Appl. Sci.*, vol. 9, no. 23, p. 5080, 2019.

[6] M. Liu, L. Liu, H. Song, Y. Hu, Y. Yi, and F. Gong, Signal estimation in underlay cognitive networks for industrial Internet of Things, *IEEE Trans. Ind. Inform.*, vol. 16, no. 8, pp. 5478–5488, 2020.

[7] M. A. Hossain, R. Md Noor, K. L. A. Yau, S. R. Azzuhri, M. R. Z'aba, I. Ahmedy, and M. R. Jabbarpour, Machine learning-based cooperative spectrum sensing in dynamic segmentation enabled cognitive radio vehicular network, *Energies*, vol. 14, no. 4, p. 1169, 2021.

[8] T. N. Do and B. An, Cooperative spectrum sensing schemes with the interference constraint in cognitive radio networks, in *Proc. 2014 Int. Symp. on Computer, Consumer and Control*, Taichung, China, 2014, pp. 1010–1013.

[9] M. Ali and H. Nam, Optimization of spectrum utilization in cooperative spectrum sensing, *Sensors*, vol. 19, no. 8, p. 1922, 2019.

[10] I. Kakalou and K. E. Psannis, Sustainable and efficient data collection in cognitive radio sensor networks, *IEEE Trans. Sustain. Comput.*, vol. 4, no. 1, pp. 29–38, 2019.

[11] D. S. Gurjar, H. H. Nguyen, and P. Pattanayak, Performance of wireless powered cognitive radio sensor networks with nonlinear energy harvester, *IEEE Sens. Lett.*, vol. 3, no. 8, pp. 1–4, 2019.

[12] B. Lyu, H. Guo, Z. Yang, and G. Gui, Throughput maximization for hybrid backscatter assisted cognitive wireless powered radio networks, *IEEE Internet Things J.*, vol. 5, no. 3, pp. 2015–2024, 2018.

[13] Z. Zhang, X. Wen, H. Xu, and L. Yuan, Sensing nodes selective fusion scheme of spectrum sensing in spectrum-heterogeneous cognitive wireless sensor networks, *IEEE Sens. J.*, vol. 18, no. 1, pp. 436–445, 2018.

[14] J. Ren, Y. Zhang, R. Deng, N. Zhang, D. Zhang, and X. Shen, Joint channel access and sampling rate control in energy harvesting cognitive radio sensor networks, *IEEE Trans. Emerg. Top. Comput.*, vol. 7, no. 1, pp. 149–161, 2019.

[15] T. Van Nguyen, T. N. Do, V. N. Q. Bao, D. B. da Costa, and B. An, On the performance of multihop cognitive wireless powered D2D communications in WSNs, *IEEE Trans. Veh. Technol.*, vol. 69, no. 3, pp. 2684–2699, 2020.

[16] A. Bagheri and A. Ebrahimzadeh, Statistical analysis of lifetime in wireless cognitive sensor network for multi-channel cooperative spectrum sensing, *IEEE Sens. J.*, vol. 21, no. 2, pp. 2412–2421, 2021.

[17] M. Liu, G. Liao, N. Zhao, H. Song, and F. Gong, Data-driven deep learning for signal classification in industrial cognitive radio networks, *IEEE Trans. Ind. Inform.*, vol. 17, no. 5, pp. 3412–3421, 2021.

[18] M. Shafiee and V. T. Vakili, Comparative evaluation approach for spectrum sensing in cognitive wireless sensor networks (C-WSNs), *Can. J. Electr. Comput. Eng.*, vol. 41, no. 2, pp. 77–86, 2018.

[19] D. Wang and Y. Song, ECCO: A novel end-to-end congestion control scheme in multi-hop cognitive radio ad hoc networks, *IEEE Trans. Cogn. Commun. Netw.*, vol. 5, no. 1, pp. 93–102, 2019.

[20] Y. Aborahama and M. S. Hassan, On the stochastic modeling of the holding time of SUs to PU channels in cognitive radio networks, *IEEE Trans. Cogn. Commun. Netw.*, vol. 6, no. 1, pp. 282–295, 2020.

[21] F. Li, K. Y. Lam, X. Li, Z. Sheng, J. Hua, and L. Wang, Advances and emerging challenges in cognitive internet-of-things, *IEEE Trans. Ind. Inform.*, vol. 16, no. 8, pp. 5489–5496, 2020.

[22] R. A. Osman and A. I. Zaki, Energy-efficient and reliable Internet of Things for 5G: A framework for interference control, *Electronics*, vol. 9, no. 12, p. 2165, 2020.

[23] M. Baniata, H. T. Reda, N. Chilamkurti, and A. Abuadbba, Energy-efficient hybrid routing protocol for IoT communication systems in 5G and beyond, *Sensors*,

vol. 21, no. 2, p. 537, 2021.
[24] M. S. Al-kahtani, L. Ferdouse, and L. Karim, Energy efficient power domain non-orthogonal multiple access based cellular device-to-device communication for 5G networks, *Electronics*, vol. 9, no. 2, p. 237, 2020.
[25] P. K. Sahoo, S. Mohapatra, and J. P. Sheu, Dynamic spectrum allocation algorithms for industrial cognitive radio networks, *IEEE Trans. Ind. Inform.*, vol. 14, no. 7, pp. 3031–3043, 2018.
[26] G. A. Gallardo, G. Jakllari, L. Canourgues, and A. L. Beylot, Statistical admission control in multi-hop cognitive radio networks, *IEEE/ACM Trans. Netw.*, vol. 26, no. 3, pp. 1390–1403, 2018.
[27] A. Patel, H. Ram, A. K. Jagannatham, and P. K. Varshney, Robust cooperative spectrum sensing for MIMO cognitive radio networks under CSI uncertainty, *IEEE Trans. Signal Process.*, vol. 66, no. 1, pp. 18–33, 2018.
[28] L. Xu, L. Cai, Y. Gao, J. Xia, Y. Yang, and T. Chai, Security-aware proportional fairness resource allocation for cognitive heterogeneous networks, *IEEE Trans. Veh. Technol.*, vol. 67, no. 12, pp. 11694–11704, 2018.
[29] T. Balachander and M. B. M. Krishnan, Carrier frequency offset (CFO) synchronization and peak average power ratio (PAPR) minimization for energy efficient cognitive radio network (CRN) for 5G wireless communication, *Wirel. Pers. Commun.*, vol. 127, no. 3, pp. 1847–1867, 2022.
[30] S. Wu, S. Shen, X. Xu, Y. Chen, X. Zhou, D. Liu, X. Xue, and L. Qi, Popularity-aware and diverse web APIs recommendation based on correlation graph, *IEEE Trans. Comput. Soc. Syst.*, vol. 10, no. 2, pp. 771–782, 2023.
[31] L. Qi, Y. Yang, X. Zhou, W. Rafique, and J. Ma, Fast anomaly identification based on multiaspect data streams for intelligent intrusion detection toward secure industry 4.0, *IEEE Trans. Ind. Inform.*, vol. 18, no. 9, pp. 6503–6511, 2022.
[32] C. Yang, X. Xu, X. Zhou, and L. Qi, Deep Q network-driven task offloading for efficient multimedia data analysis in edge computing-assisted IoV, *ACM Trans. Multimedia Comput. Commun. Appl.*, vol. 18, no. 2, pp. 1–24, 2022.

Thulasiraman Balachander received the bachelor degree in information technology from Madurai Kamraj University, India in 2003, and the MS degree in advanced computing from SASTRA University, India in 2006. He received the PhD degree in computer science and engineering from SRM Institute of Science and Technology, India in 2022. He is currently working as an assistant professor in SRM Institute of Science and Technology, India. He has published research publications in various reputed national & international journals and conferences. His research areas include cognitive radio networks, 5G, block chain technology, Internet of Things (IoT), Malware analysis, and Cyber security.

Gautam Srivastava received the MS and PhD degrees in computer science from University of Victoria, Canada in 2006 and 2012, respectively. He is a professor of computer science at Brandon University, Canada. In his 10-year academic career, he has published 400 papers in high-impact conferences in many countries and high-status journals. He is an editor of several international scientific research journals, including *IEEE Transactions on Industrial Informatics, IEEE Transactions on Computational Social Systems*, and *IEEE Internet of Things Journal*.

Kadiyala Ramana is currently working as an associate professor and a head of Department of Artificial Intelligence and Data Science, Chaitanya Bharathi Institute of Technology (Autonomous), India. During 2007–2021, he was an assistant professor in Department of Information Technology at Annamacharya Institute of Technology and Sciences (Autonomous), India. He received the bachelor degree in information technology in 2007 from Jawaharlal Nehru Technological University, India, and the MS degree in information technology in 2011 from Sathyabhama University, India. He received the PhD degree in philosophy in November 2019 from SRM University, India. His research areas are distributed systems, parallel and distributed systems, software defined networking, cluster computing, and web technologies. He has published more than 50 papers in reputed international journals and also attended various international conferences. He is a reviewer of several international journals and program committee member of various international conferences. He is a life time member of IAENG, IE(I), ISTE, and IACSIT.

Thippa Reddy Gadekallu currently works as an associate professor at School of Information Technology and Engineering, Vellore Institute of Technology, India. He obtained the bachelor degree in computer science and engineering from Nagarjuna University, India in 2003, the MS degree in computer science and engineering from Anna University, India in 2011, and the PhD degree from Vellore Institute of Technology, India in 2017. He has more than 14 years of experience in teaching. He has more than 150 international/national publications in reputed journals and conferences. Currently, his research areas include machine learning, Internet of Things, deep neural networks, blockchain, and computer vision.

Rasineni Madana Mohana is a senior member of IEEE and works as a professor in Department of Artificial Intelligence & Data Science at Chaitanya Bharathi Institute of Technology, India, and he is also an adjunct lecturer at Botho University, India. He has more than 19 years of extensive experience in research and teaching. His research areas are artificial intelligence, machine learning, data science, big data analytics, formal languages & automata theory, compiler design, database management systems, and data mining.